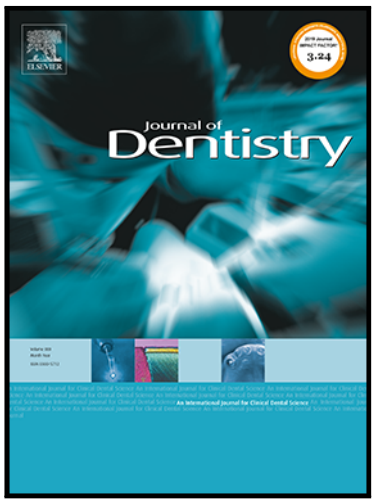

Impact of the superimposition methods and the designated comparison area on accuracy analyses in dentate models

Alvaro Limones , Pedro Molinero-Mourelle , Gülce Çakmak , Samir Abou-Ayash , Silvia Delgado , Juan Antonio Martínez Vázquez de Parga , Alicia Celemín

PII: S0300-5712(24)00109-X
DOI: https://doi.org/10.1016/j.jdent.2024.104939
Reference: JJOD 104939

To appear in: *Journal of Dentistry*

Received date: 1 October 2023
Revised date: 25 February 2024
Accepted date: 12 March 2024

Please cite this article as: Alvaro Limones , Pedro Molinero-Mourelle , Gülce Çakmak , Samir Abou-Ayash , Silvia Delgado , Juan Antonio Martínez Vázquez de Parga , Alicia Celemín , Impact of the superimposition methods and the designated comparison area on accuracy analyses in dentate models, *Journal of Dentistry* (2024), doi: https://doi.org/10.1016/j.jdent.2024.104939

Title: Impact of the superimposition methods and the designated comparison area on accuracy analyses in dentate models

Running title: Superimposition methods accuracy in dentate models

Alvaro Limones[a], Pedro Molinero-Mourelle[a,b], Gülce Çakmak[a], Samir Abou-Ayash[a], Silvia Delgado[a], Juan Antonio Martínez Vázquez de Parga[a*] & Alicia Celemín[a*]

[a]Department of Conservative Dentistry and Prosthodontics, Faculty of Odontology, University Complutense of Madrid, Madrid, Spain.

[b]Department of Reconstructive Dentistry and Gerodontology, University of Bern, Bern, Switzerland.

*These authors have contributed equally to this work as senior author.

CORRESPONDENCE

Alvaro Limones, Department of Conservative Dentistry and Prosthodontics, Faculty of Odontology, University Complutense of Madrid, Plaza Ramón y Cajal, Madrid 28040, Spain. Email: alimones@ucm.es

Pedro Molinero-Mourelle, Department of Reconstructive Dentistry and Gerodontology, University of Bern, Bern, Switzerland. Email: pedro.molineromourelle@unibe.ch

ABSTRACT

Objectives: To measure the impact of superimposition methods and the designated comparison area on accuracy analyses of dentate models using an ISO-recommended 3-dimensional (3D)

metrology-grade inspection software (Geomagic Control X; 3D Systems; Rock Hill, South Carolina; USA).

Materials and methods: A dentate maxillary typodont scanned with a desktop scanner (E4; 3 Shape; Copenhagen; Denmark) and an intraoral scanner (Trios 4; 3 Shape; Copenhagen; Denmark) was used as reference. Eight groups were created based on the core features of each superimposition method: landmark-based alignment (G1); partial area-based alignment (G2); entire tooth area-based alignment (G3); double alignment combining landmark-based alignment with entire tooth area-based alignment (G4); double alignment combining partial area-based alignment with entire tooth area-based alignment (G5); initial automated quick pre-alignment (G6); initial automated precise pre-alignment (G7); and entire model area-based alignment (G8). Diverse variations of each alignment and two regions for accuracy analyses (teeth surface or full model surface) were tested, resulting in a total of thirty-two subgroups (n=18). The alignment accuracy between experimental and reference meshes was quantified using root mean square (RMS) error as trueness and its repeatability as precision. The descriptive statistics, a factorial repeated measures analysis of variance (ANOVA) and a post hoc Tuckey multiple comparison tests were used to analyze the trueness, and precision (α = .05).

Results: A total of 576 superimpositions were performed. The unique partial area-based superimposition method demonstrated the least precise alignment and was the sole group to exhibit a significant difference (p<.001). Automated initial pre-alignments demonstrated similar accuracy to other superimposition methods (p>.05). Double alignments did not result in accuracy improvement (p>.05). The designated comparison area displayed differences in both trueness (p<.001) and precision (p<.001), leading to an 8±4μm discrepancy between selecting the teeth surface or full model surface.

Conclusions: The superimposition method choice within the tested software did not impact accuracy analyses, except when the alignment relies on a unique and reduced area, such as the palatal rugae, a single tooth, or three adjacent teeth on one side.

Clinical Significance: The superimposition method choice within the tested ISO-recommended 3D inspection software did not impact accuracy analyses.

Keywords: Intraoral scanner; Alignment; Superimposition; Best-fit; Digital dentistry

1. INTRODUCTION

In recent years, the assessment of digital dentistry interventions through accuracy analyses has notably gained prominence. Accuracy analyses in adherence to ISO 5725–1:1994 (International Organization for Standardization) and ISO 20896-1:2019, includes both trueness and precision [1, 2]. Trueness refers to a scanner's capability to replicate a dental arch faithfully, without any deformation or distortion, aiming to reproduce its true form as accurately as possible. Conversely, precision pertains to the consistency and degree of similarity among images obtained through repetitive scanning procedures conducted under identical conditions. These assessments need to acquire a reference mesh, either through scanning a master model using desktop or industrial scanners, or using a digital design created by Computer-Aided Design (CAD) software. Subsequent experimental meshes are formed based on specific research objectives and superimposed onto the reference mesh for evaluation. Traditionally, three mesh superimposition methods have been employed: landmark-based alignment, partial area-based alignment, and entire area-based alignment [3, 4]. Landmark-based and partial area-based alignments require the operator's expertise, involving manual selection of common landmarks or partial areas [5].

Conversely, entire area-based alignments are more replicable, objective, and less dependent on the operator. Area-based alignments commonly use the Gaussian best-fit algorithm, also known as the "Iterative Closest Point" (ICP) algorithm, to automatically integrate two-point clouds and interactively minimize measurement errors [6]. Upon superimposing the test mesh over the reference mesh, 2-dimensional (2D) measurements comparing the linear and angular deviations of two lines on cross-sections, or 3-dimensional (3D) measurements comparing the distance between two 3D-surfaces through the root mean square (RMS) error calculation, are typically performed. This methodology has several applications such as: manufacturing accuracy assessment [7 - 14], analyzing tooth wear progression [15], assessing intraoral or facial scanner accuracy [16, 17], investigating their influencing factors [18], or recording dynamic occlusion [19].

Nevertheless, the impact of the chosen 3D inspection software [20 - 22], superimposition methods [23, 24], or the designated area for analysis on these evaluations remains uncertain. Moreover, currently there is methodological heterogeneity in digital dental research [17] presenting a challenge and a burden in establishing standardized protocols for consistent comparisons among studies. Consequently, further research is needed to clarify their impact, refine methodologies for enhanced accuracy, and ensure consistency in digital dentistry evaluation to strengthening the evidence to provide robust recommendations in daily clinical settings.

Therefore, the primary objective of this study was to measure the impact of the superimposition method and the designated comparison area on accuracy analyses in dentate models. The secondary objectives of this study were:

1. Measure the accuracy of initial pre-alignments.
2. Measure the impact of the spacing or quantity of landmarks on landmark-based alignments.

3. Measure the impact of the size or location of the selected area on partial area-based alignments.
4. Measure the accuracy of double alignments compared to single alignments.
5. Measure the impact of solely utilizing the region of interest in entire area-based alignment, specifically comparing entire tooth area-based alignment with entire model area-based alignment.

The general null hypothesis of this study was that there would be no significant differences in accuracy among mesh superimposition methods or selected comparison areas.

2. MATERIALS AND METHODS

2.1. Study design

This comparative in vitro study was performed at the XXXX. Ethics approval was not required from the Ethics Committee Research for this in vitro study since no humans' samples were used.

A sample size calculation was determined based on the research conducted by Revilla-Leon et al. 2023 [3] with a mean ± SD of 170 ±14µm for the landmark-based group and 160 ±1µm for the entire area-based alignment group with a 1:1 sampling rate, an alpha error of 5%, an 80% power, and two-sided paired-mean hypothesis test. Upon calculation, 18 specimens per subgroup were determined as necessary for the study.

2.2 Study set-up

A maxillary dentate typodont (Frasaco ANKA-4; Frasaco, Germany) was used to mimic a healthy dentate individual. For the digitization, a reference cast was scanned with a desktop laboratory scanner (E4; 3 Shape, Copenhagen, Denmark) following the manufacturer's instructions. The obtained reference scan (control) was exported in a standard tessellation language

(STL) file format. The same model was scanned using an intraoral scanner (IOS) (Trios 4; 3 Shape; Copenhagen; Denmark). The chosen IOS had been previously calibrated before starting and every six scans following the manufacturer's recommended protocol. To ensure consistent lighting conditions at 1000 lux, the data collection was performed in a windowless room, using a light-emitting diode (LED) panel light (660 Pro RGB; Neewer; Shenzhen; China) [26-28]. The light intensity was measured using a luxmeter (LX1330B Light Meter; Dr. Meter Digital Illuminance, Union City, USA). The intraoral digital scans were conducted by an experienced operator (P.M.-M.) with more than 5 years of prior expertise working with IOSs. A 20-minute break was done after six completed digital scans to prevent operator fatigue. The scanning started at the occlusal surface of the right second molar, and then it traversed all occlusal surfaces along the path until reaching the contralateral second molar. Subsequently, the scanner's orientation was altered to capture the lingual surfaces, starting from the left second molar and extending to the right. The process was repeated on the buccal side in the opposite direction to complete the scan. The scans were thoroughly visually inspected to ensure their accurate and satisfactory registration. This procedure was repeated to obtain 18 test scans, which were exported in an STL file format. No cleaning of the mesh files was conducted before importing them into the 3D inspection software.

2.3 STL files superimposition

The STL files were superimposed by using a 3D inspection software (Geomagic Control X, v.2022. 3D Systems, Rock Hill, South Carolina, USA) onto the reference model's STL through eight distinct alignment methods, resulting in the following groups:

- A landmark-based alignment group (G1).
- A partial area-based alignment group (G2).
- An entire tooth area-based alignment group (G3)

- A two-stage double alignment group consisting of a primary landmark-based alignment followed by a secondary entire tooth area-based alignment (G4)
- A two-stage double alignment group consisting of a primary partial area-based alignment followed by a secondary entire tooth area-based alignment (G5).
- An initial automated quick pre-alignment group (G6).
- An initial automated precise pre-alignment group (G7),
- The entire model area-based alignment (G8).

The superimposition methods preceded an initial automated quick pre-alignment stipulated by the software, except group 7. All area-based alignments were grounded in the Gaussian best-fit algorithm.

2.4 Accuracy evaluation

For a more comprehensive assessment of landmark-based alignments (G1), two factors – the distance between points and the quantity of points – were investigated through sub-analyses. Three subgroups underwent analysis with the rationale of examining whether modifications in the distance between point placements or the number of points could impact the accuracy of the landmark-based alignment:

- Subgroup G1A (Fig. 1.1a) thus utilized three closely positioned points,
- Subgroup G1B (Fig. 1.1b) involved three points widely separated from each other, and
- Subgroup G1C (Fig. 1.1c) employed seven points across the arch. These points were strategically located at the most consistent areas: the cingulum of the anterior teeth, the mesial fossa of the premolars, and the central fossa of the molars.

For a more comprehensive assessment of partial area-based alignments (G2), two factors – the designated area size and its location – were investigated through sub-analyses. Three subgroups

underwent analysis with the rationale of examining whether modifications in the area size corresponding to 1 or 3 teeth, or the location on teeth or mucosa could potentially affect the accuracy of partial area-based alignments:

- Subgroup G2A (Fig. 1.2a) focused solely on the area of a single tooth.
- Subgroup G2B (Fig. 1.2b) encompassed three adjacent teeth on the same side.
- Subgroup G2C (Fig. 1.2c) centered around the palatal rugae.

The designated area in the entire tooth area-based alignment (G3), entailed a meticulous selection of the teeth as the region of interest, deliberately excluding the gingival area for the alignment (Fig. 1.3).

For a comprehensive assessment of double alignments in two-steps, this study explored the initial application of landmark-based alignments (same from subgroups G1A to G1C), and partial area-based alignments (same from subgroups G2A to G2C) in a first step, followed by a second alignment based on the entire tooth area-based alignment in a second step. The rationale behind this assessment was to assess whether double alignments show any substantial accuracy differences compared to single alignments. Consequently, six subgroups were established:

- Subgroup G4A (Fig. 1.4a) implemented an initial alignment using three closely positioned points, followed by a secondary entire tooth area-based alignment.
- Subgroup G4B (Fig. 1.4b) employed three widely separated points in the initial alignment, followed by a secondary entire tooth area-based alignment.
- Subgroup G4C (Fig. 1.4c) used an initial alignment involving seven points across the arch, followed by a secondary entire tooth area-based alignment.
- Subgroup G5A (Fig. 1.5a), focusing on the area of a single tooth in the initial alignment, followed by a secondary entire tooth area-based alignment.

- Subgroup G5B (Fig. 1.5b) encompassed a broader area involving three adjacent teeth on the same side in the initial alignment, followed by a secondary entire tooth area-based alignment.
- Subgroup G5C (Fig. 1.5c) centered on the palatal rugae in the initial alignment, followed by a secondary entire tooth area-based alignment.

For a comprehensive assessment of initial alignments required by the inspection software, two pre-alignment options were investigated – initial quick alignment option (G6, Fig. 1.6), and initial precise alignment option (G7, Fig. 1.7). The rationale for this assessment was to determine the accuracy attained by the initial pre-alignment, a requisite for the inspection software, and to discern if there were notable accuracy differences compared to alternative superimposition methods.

The designated area in the entire model area-based alignment (G3), involved using the entire mesh of the model for the alignment (G8; Fig. 1.8), without specifically selecting any landmarks or areas of interest.

Two comparison areas, the tooth area, or the entire model area (excluding the model base), were designated and analyzed to assess all alignments. The rationale of this evaluation was to analyze how the chosen area for analysis influences accuracy analyses. It entailed analyzing all subgroups designating the tooth area, denoted with the 'T' label, and all subgroups designating the entire model area, denoted with the 'M' label.

2.5 Study outcomes

The primary outcome was to evaluate the accuracy, assessed by trueness and precision in microns (μm). Trueness was defined as the average RMS error discrepancies on the superimposition of the reference and experimental scans [1, 2]. Precision was detailed as the RMS error fluctuations per each group or standard deviation (SD) [1, 2] and using the following formulae $\mathrm{RMS} = \sqrt{\frac{\sum_{i=1}^{n}(X_{1,i} - X_{2,j})^2}{n}}$ where $X_{1,i}$ are the reference data, $X_{2,j}$ are the scan data, and n

indicated the total number of measurement points analyzed in each examination. The calculations of discrepancies for each group were employed for data analysis. Color-coded maps were employed to illustrate the discrepancies identified by the software between each mesh pair comparison. These visual representations used a color gradient scale to depict the directionality of deviations: cool shades indicated inward deviations, warm shades represented outward deviations, and minimal deviations were denoted by green hues (Fig. 2). The mesh densities of both the reference STL and the intraoral scanner STLs were determined by counting the number of triangles and vertices (Meshmixer, Autodesk, Mill Valley, USA).

2.6 Statistical analysis

A blind statistical analysis was performed using a coded default Excel spreadsheet to ensure the prevention of data manipulation or hypothesis testing. After the statistical analysis, the coding was revealed to edit tables and graphs. Descriptive statistics (mean values, standard deviations, medians, and interquartile range) of variables were calculated. The results of the Shapiro–Wilk tests indicate that the trueness and precision data exhibited a normal distribution ($p > .05$). Consequently, a factorial repeated measures analysis of variance ANOVA and a post hoc Tuckey multiple comparison tests were used to analyze the trueness, and precision ($\alpha = .05$) at both the group and subgroup levels. Data analysis and visualization were conducted utilizing the statistical software program STATA (v 17.0; StataCorp LP, TX, USA).

3. RESULTS

A total of 576 superimpositions were done and were grouped into eight groups and subdivided into 32 subgroups. Tables 1 and 2 shows trueness and precision values obtained by group and subgroup, ranked by alignment accuracy from highest to lowest. Mean differences

across subgroups are presented in Table 3. Statistical analysis using factorial ANOVA revealed a significant variance in trueness and precision values among the evaluated groups (p<.001) (Fig. 3; Table 4). Post hoc Tukey tests indicated significant differences in trueness and precision between G2 and other superimposition groups (p<.001) (Fig. 4). Specifically, the subgroup analysis identified G2A, G2B, and G2C as significant contributors to this distinction (p<.001). However, there were no significant differences in terms of trueness and precision among other superimposition methods (p<.001). The comparison area choice had a significant impact on both trueness (p<.001) and precision (p<.001), resulting in an 8±4 µm difference in trueness and precision between selecting the tooth area and the complete mesh (Table 4).

The initial alignment required by the inspection software (quick or precise alignment) did not show any substantial accuracy differences compared to other superimposition method (p=.999), except G2. On the landmark-based alignment, no significant accuracy differences were found on the distance or quantity of the alignment points (G1A, G1B, and G1C), nor in the use of two-stage mesh superimposition strategy (p=.999) (G1 and G4). On the partial area-based alignment, no significant accuracy variations were observed related to the size or location of the designated area (p=.999) (G2A, G2B, and G2C) nor in the use of two-stage mesh superimposition strategy (p=.999) (G2 and G5). No significant accuracy differences were found between the entire tooth area-based alignment and the entire model area-based alignment (p=.999) (G3 and G8).

The reference scan conducted with the desktop scanner comprised 173,184 triangles and 86,574 vertices. The intraoral scans displayed approximately 3.3 times more triangles, totaling 575,559 triangles (±43,092), and vertices reaching 289,545 (±21,743).

4. DISCUSSION

Based on the findings of this in-vitro study, the general null hypothesis was partially accepted. While the alignment accuracy based on the entire tooth area-based alignment exhibited a greater mean value of 94±15μm compared to other groups, this difference did not attain statistical significance, except when compared to the unique partial area-based alignment method. Notable differences in accuracy (trueness and precision), were observed between this method and the remaining mesh superimposition methods. The inspection software program's initial pre-alignment alternatives, whether quick or precise, did not show significant differences in accuracy compared to the other superimposition methods, except for the unique partial area-based alignment method. Furthermore, the use of quick or precise mode in automated initial pre-alignments yielded similar accuracy. In the landmark-based alignment, the increase in points or their spatial separation did not result in accuracy enhancements. In the partial areas-based alignment, neither modifying the area size nor its location yield accuracy enhancements. Besides, a single or a double mesh superimposition method by using landmark based alignment or area-based alignment did not differ in accuracy. The entire tooth area-based alignment resulted in similar accuracy compared to that of the entire model area-based alignment. Considering the obtained data, it could be interpreted that the mesh superposition methods that were analyzed had a limited impact on the accuracy analysis of dentate models. The exception was the partial area-based alignment, which focused on a unique and reduced area. A potential explanation for the increased discrepancy in results obtained with partial area-based alignment could be attributed to the unilateral selection of a specific area. Different results could be obtained if bilateral selection of partial areas were performed. Regarding color maps, a heterogeneous deviation pattern and red areas have been observed in the opposite arch to the alignment area, which indicates outward deviations. In contrast, green or yellow areas showed deviations within the tolerance range, or a slight outward deviation in the alignment area

(Figure 2). Entire tooth area-based alignment, which includes alignment with bilateral tooth areas, resulted in more homogenous deviation pattern with prominent green areas (acceptable deviation).

Unlike to the present study results, prior in-vitro studies showed that partial area-based alignment achieved the highest level of alignment accuracy [3, 16]. This could be attributed to the fact that Revilla-León et al., adopted a multiple bilateral partial areas approach for the partial area-based alignment, which differs from our study's set-up on a single area [3]. This trend might be explained by the potential difficulties entire area-based alignments face when dealing with artifacts arising from scanning errors occur due to multiple rescans, scanning pauses, incorrect scanning patterns, or a large scan length resulting from the data stitching process [29]. Therefore, in certain situations, the superimposition method choice that relies on points or multiple partial areas free from artifacts may lead to a more accurate alignment.

Despite the subjectivity and operator-dependent nature of these methods, this study showed similar outcomes between landmark-based and entire tooth or entire model area-based alignments, or even double alignments. It is important to note that the measurements were conducted by a skilled operator, and the results may vary with less experienced ones. A previous study has reported that the operator had an impact on the measured deviations when different 3D analysis software programs [9]. Highlighting the need for experienced operators to obtain consistent measurements. This aspect is particularly crucial during the selection of points and areas, ensuring their repeatability, and aiming for a distinctive and well-defined feature, such as the edge of a dental groove or a clearly recognizable cusp. Moreover, it is essential to avoid selecting regions with surface irregularities, which could potentially complicate the alignment process.

The present study's findings showed that the accuracy achieved through the initial pre-alignment, that is a requested step in the 3D inspection software tested, is comparable to that

achieved by other superimposition methods. It is difficult to directly compare the present study results with previous studies because many of the previous studies did not mention if they applied an initial (quick or precise) pre-alignment or employed a software version that did not allow for these options. O'Toole et al., performed comparison study of alignment procedures, including best-fit alignment (referred to entire area-based alignment in the present study), landmark-based alignment, and reference best-fit alignment (reducing data set use by restricting alignment to operator-identified sections and is referred to partial area-based alignment in the present study) was done [4]. In contrast with the present study, the authors reported that the reference best-fit alignment, which corresponds to groups G2, G3, G4, and G5 of the present study, showed lower alignment errors and higher accuracy. Otherwise, the authors reported that entire area-based alignment and landmark-based alignment algorithms underestimated the size of the defect. The difference between this study and the present study may be due to the size of the meshes. O'Toole et al. compared natural molar teeth, which may have reduced mesh size compared to the dentate model used in the present study. Considering the present study, especially while analyzing bigger structures with more meshes, quick alignment can be recommended over precise alignment, which might provide a faster 3D analysis.

Peroz et al., (2021) [21] explored various alignment algorithms on entire area-based alignments, such as the Gauss best-fit algorithm and the exterior, median, or interior Chebyshev best-fit algorithm. However, the aim of the study was not to assess the complex internal algorithms of each software, as it was done in our study specifically using the Gauss best-fit algorithm for all area-based alignments. Nevertheless, this might be an additional factor to consider as different 3D inspection software may produce different measurements [20 - 22]. Additionally, this study discusses how mesh density may be a confounding factor in RMS analyses for evaluating 3D

discrepancies between digital meshes [21]. In the present study, the maximum mesh density available was used without making modifications to the original STL files, which remained intact and were directly exported to the metrology-grade inspection software.

The clinical implications of this study lie in understanding how superimposition methods and designated comparison areas affect accuracy analyses when evaluating interventions in digital dentistry. The obtained data suggested that future research could designate comparison areas that align with the specific area of interest, avoiding the assessment of complete models, as it has been observed to decrease accuracy. Additionally, this study dismisses the notion that diversity in superimposition methods is a reason for inconsistency among study results and may not be a crucial factor to consider when using this ISO-recommended software. Moreover, it offers valuable insights by warning against the inefficacy of double alignments, excessive point marking, or selecting overly extensive areas, thereby guiding future research in this field.

The current study has certain limitations, including the examination of a single inspection software and the exclusive focus on a maxillary model. In the present study, ISO-recommended metrology-grade software program was used with the RMS methodology. Different results may be obtained when different deviation measurement methods are used [30]. Therefore, future studies, should include other software programs and additional metrology-grade programs and nonmetrology-grade freeware programs. The results should be approached with caution, considering factors such as software version upgrades and the operator's level of experience. It was previous reported that not using an industrial scanner to acquire a reference scan can be a limitation, nevertheless a recent study supports the use of desktop scanner as control like in the present study showed similar precision compared to an industrial grade optical scanner [31].

5. CONCLUSION

The superimposition method choice, within the tested ISO-recommended inspection software, did not impact accuracy analyses, except when the alignment relies on a unique and reduced mesh area, such as the palatal rugae, a single tooth, or three adjacent teeth on one side; therefore, one should refrain from using this superimposition method. Besides, the findings show critical insights for future research, especially in considering the following practical implications for accuracy evaluation.

1. Automated initial pre-alignments exhibited comparable accuracy in comparison to other superimposition methods.
2. Increasing the quantity of points or modifying their spatial distribution in landmark-based alignments did not result in improved accuracy.
3. Adjusting the size or position of a specific partial area on one side in the partial area-based alignment did not yield accuracy improvements.
4. Double mesh superimposition method, using either landmark-based or area-based alignment, did not show accuracy improvements.
5. The alignment based on the entire tooth area produced similar accuracy to those made with entire model area-based alignment, although it is important to interpret this cautiously, given the in-vitro nature of this study.

REFERENCES

[1] International Organization for Standardization. ISO 5725-1:1994. (1994). Accuracy (trueness and precision) of measurement methods and results— Part 1: General principles and definitions. Retrieved January 2, 2020, from https://www.iso.org/obp/ui/#iso:std:iso:5725:-1:ed-1:v1:en

[2] International Organization for Standardization. ISO 20896-1:2019. (2019). Dentistry—Digital impression devices—Part 1: Methods for assessing accuracy. Retrieved January 2, 2020, from https://www.iso. org/standard/69402.html

[3] M. Revilla-León, A. Gohil, A.B. Barmak, A. Zandinejad, A.J. Raigrodski, J. Alonso Pérez-Barquero, J. Best-Fit Algorithm Influences on Virtual Casts' Alignment Discrepancies. J. Prosthodont. (2023) 32(4), 331–339. doi:10.1111/jopr.13537.

[4] S. O'Toole, C. Osnes, D. Bartlett, A. Keeling. Investigation into the accuracy and measurement methods of sequential 3D dental scan alignment. Dental. Mat. (2019) 35(3), 495-500. doi:10.1016/j.dental.2019.01.012.

[5] K. Becker, B. Wilmes, C. Grandjean, D. Drescher. Impact of manual control point selection accuracy on automated surface matching of digital dental models. Clin. Oral. Invest. (2018) 22(2), 801-810. doi:10.1007/s00784-017-2155-6.

[6] S. Rusinkiewicz, M. Levoy. Efficient variants of the ICP algorithm. International Conference on 3-D Digital Imaging and Modeling, (2001) 145-152. doi: 10.1109/IM.2001.924423.

[7] G. Çakmak, D Agovic, M.B. Donmez, Ç. Kahveci, M.S. de Paula, M. Schimmel, B. Yilmaz. (2023). Effect of number of supports and build angle on the fabrication and internal fit accuracy of additively manufactured definitive resin-ceramic hybrid crowns. J. Dent. (2023) 134, 104548. doi:10.1016/j.jdent.2023.104548.

[8] G. Çakmak, M.B. Donmez, C Akay, M.S. de Paula, F.G. Mangano, S Abou-Ayash, B Yilmaz. Effect of measurement techniques and operators on measured deviations in digital implant scans. J. Dent. (2023) 130, 104388. doi:10.1016/j.jdent.2022.104388.

[9] G. Cakmak, V.R. Marques, M.B. Donmez, W.E. Lu, S. Abou-Ayash, Yilmaz B. (2022). Comparison of measured deviations in digital implant scans depending on software and operator. J. Dent. (2022) 122, 104154. doi:10.1016/j.jdent.2022.104154.

[10] G. Çakmak, A.M. Rusa, M.B. Donmez, C. Akay, Ç. Kahveci, M. Schimmel, B. Yilmaz. (2022). Trueness of crowns fabricated by using additively and subtractively manufactured resin-based CAD-CAM materials. J. Prsoth. Dent. (2022) S0022-3913(22)00690-4. doi:10.1016/j.prosdent.2022.10.012.

[11] D.Ö. Dede, G Çakmak, M.B. Donmez, A.S. Küçükekenci, W.E. Lu, A.A. Ni, B. Yilmaz. (2023). Effect of analysis software program on measured deviations in complete arch, implant-supported framework scans. J. Prosthet. Dent. (2023) S0022-3913(23)00436-5. doi:10.1016/j.prosdent.2023.06.028.

[12] M.B, Donmez, B. Yilmaz, H.I. Yoon, Ç. Kahveci, M Schimmel, G. Effect of computer-aided design and computer-aided manufacturing technique on the accuracy of fixed partial denture patterns used for casting or pressing. J. Dent. (2023) 130, 104434. doi:10.1016/j.jdent.2023.104434.

[13] B.Y. Yu, K. Son, K.B. Lee, K. (2021). Evaluation of intaglio surface trueness and margin quality of interim crowns in accordance with the build angle of stereolithography apparatus 3-dimensional printing. J. Prosth. Dent. (2021) 126(2), 231–237. doi:10.1016/j.prosdent.2020.04.028. doi:10.1016/j.jdent.2023.104434.

[14] H. Lerner, K. Nagy, N. Pranno, F. Zarone, O. Admakin, F. Mangano. Trueness and precision of 3D-printed versus milled monolithic zirconia crowns: An in vitro study. J. Dent. (2021) 113, 103792. doi:10.1016/j.jdent.2021.103792.

[15] C. Wulfman, V. Koenig, A.K. Mainjot. Wear measurement of dental tissues and materials in clinical studies: A systematic review. Dental. Mat. (2018) 34, 825-850. doi:10.1016/j.dental.2018.03.002.

[16] M. Revilla-León, J.A. Pérez-Barquero, B.A. Barmak, R. Agustín-Panadero, L. Fernández-Estevan, W. Att. Facial scanning accuracy depending on the alignment algorithm and digitized surface area location: An in vitro study. J. Dent. (2021) 110, 103680. doi:10.1016/j.jdent.2021.103680.

[17] V. Vitai, A. Németh, E. Sólyom, L.M. Czumbel, B. Szabó, R. Fazekas, G. Gerber, P. Hegyi, P. Hermann, J. Borbély. Evaluation of the accuracy of intraoral scanners for complete-arch scanning: A systematic review and network meta-analysis. J. Dent. (2023) 137, 104636. doi:10.1016/j.jdent.2023.104636.

[18] A.L. Carneiro Pereira, M.R. Souza Curinga, H.V. Melo Segundo, A. da Fonte Porto Carreiro. (2023). Factors that influence the accuracy of intraoral scanning of total edentulous arches rehabilitated with multiple implants: A systematic review. J. Prosthet. Dent. (2023) 129(6), 855-862. doi:10.1016/j.prosdent.2021.09.001.

[19] L. Li, H. Chen, W. Li, Y. Wang, & Y. Sun. (2023). Design of wear facets of mandibular first molar crowns by using patient-specific motion with an intraoral scanner: A clinical study. J. Dent. (2023) 129(5), 710–717. doi:10.1016/j.prosdent.2021.06.048.

[20] B. Yilmaz, V.R. Marques, M.B. Donmez, A.R. Cuellar, W.E. Lu, S. Abou-Ayash, G. Çakmak. (2022). Influence of 3D analysis software on measured deviations of CAD-CAM resin crowns from virtual design file: An in-vitro study. J. Dent. (2022) 118, 103933. doi:10.1016/j.jdent.2021.103933.

[21] S. Peroz, B.C. Spies, U. Adali, F. Beuer, C. Wesemann. Measured accuracy of intraoral scanners is highly dependent on methodical factors. J. Prosth. Res. (2022) 66, 318–325. doi:10.2186/jpr.JPR_D_21_00023.

[22] K. Son, W.S. Lee, K.B, Lee. Effect of Different Software Programs on the Accuracy of Dental Scanner Using Three-Dimensional Analysis. Int. J. Envirom. Res. Pub. Health. (2021) 18(16), 8449. doi:10.3390/ijerph18168449.

[23] T. Joda, U. Brägger, G. Gallucci. Systematic literature review of digital three dimensional superimposition techniques to create virtual dental patients. Int. J. Oral. Maxillofac. Implants. 30 (2015) 330-337. doi:10.11607/jomi.3852.

[24] H. Yilmaz, H Arınç. G Çakmak, G. Atalay, S. M.B. Donmez, A.M. Kökat, B. Yilmaz. Effect of scan pattern on the scan accuracy of a combined healing abutment scan body system. J. Prosthet. Dent. (2022) S0022-3913(22)00067-1. doi:10.1016/j.prosdent.2022.01.018.

[26] M. Revilla-León, P. Jiang, M. Sadeghpour, W. Piedra-Cascón, A. Zandinejad, M. Özcan, V.R. Krishnamurthy. Intraoral digital scans: Part 2-influence of ambient scanning light conditions on the mesh quality of different intraoral scanners. J Prosthet Dent. (2020) 124(5):575-580. doi:10.1016/j.prosdent.2019.06.004.

[27] M. Revilla-León, S.G. Subramanian, W. Att, V.R. Krishnamurthy. (2021). Analysis of different illuminance of the room lighting condition on the accuracy (trueness and precision) of an intraoral scanner. J. Prosthodont. (2021) 30(2), 157–162. doi:10.1111/jopr.13276.

[28] M. Revilla-León, S.G. Subramanian, M. Özcan, V.R. Krishnamurthy. Clinical study of the influence of ambient light scanning conditions on the accuracy (trueness and precision) of an intraoral scanner. J. Prosthodont. (2020) 29(2), 107–113. doi:10.1111/jopr.13135.

[29] A. Yehia, A. Abo El Fadl, O. El Sergany, K. Ebeid, K. (2023). Effect of different span lengths with different total occlusal convergences on the accuracy of intraoral scanners. J. Prosthodont. (2023) doi:10.1111/jopr.13686.(2023)

[30] B.B. Yatmaz, S. Raith, S. Reich. (2021). Trueness evaluation of digital impression: The impact of the selection of reference and test object. J. Dent. (2021) 111, 103706. doi:10.1016/j.jdent.2021.103706.

[31] D. Borbola, G. Berkei, B. Simon, L. Romanszky, G. Sersli, M. DeFee, W. Renne, F. Mangano, J. Vag. (2021). In vitro comparison of five desktop scanners and an industrial scanner in the evaluation of an intraoral scanner accuracy. J. Dent. 129:104391. doi: 10.1016/j.jdent.2022.104391.

TABLES

TABLE 1. Root mean square (RMS) error datasets for each superposition method by groups, ordered from highest to worst fit; N = number of analyzed points.

Group	N	Trueness (µm)						Precision (µm)					
		Mean	±	SD	Median	±	IQR	Mean	±	SD	Median	±	IQR
Entire tooth area-based alignment	36	94	±	15	93	±	20	93	±	15	92	±	20
Entire model area-based alignment	36	94	±	15	92	±	20	94	±	15	92	±	20
Initial precise alignment	36	94	±	15	92	±	19	93	±	15	92	±	19
Initial quick alignment	36	94	±	15	92	±	19	93	±	15	92	±	19
Landmark-based alignment	108	94	±	15	92	±	19	93	±	15	92	±	19
Two-stage: Landmark-based + Entire tooth area-based alignments	108	94	±	15	93	±	22	94	±	15	92	±	22
Two-stage: Partial area-based + Entire tooth area-based alignments	108	94	±	15	93	±	22	94	±	15	92	±	22
Partial area-based alignment	108	116	±	23	110	±	27	113	±	24	109	±	30

TABLE 2. Root mean square (RMS) error datasets for each superposition method by subgroups, ordered from highest to worst fit; N = number of times superimposed. G1A: 3 close-point landmark-based alignment; G1B: 3 distant-point landmark-based alignment; G1C: 7-point landmark-based alignment; G2A: partial area-based alignment of one tooth; G2B: partial area-based alignment of three adjacent teeth; G2C: partial area-based alignment of the palatal rugae; G3: entire tooth area-based alignment; G4A: primary 3 close-point landmark-based alignment followed by a secondary entire tooth area-based alignment; G4B: primary 3 distant-point landmark-based alignment followed by a secondary entire tooth area-based alignment; G4C: primary 7-points landmark-based alignment followed by a secondary entire tooth area-based alignment; G5A: primary partial tooth area-based alignment of one tooth followed by a secondary entire tooth area-based alignment; G5B: primary partial area-based alignment of three adjacent teeth followed by a secondary entire tooth area-based alignment; G5C: primary partial area-based alignment of the palatal rugae followed by a secondary entire tooth area-based alignment; G6: quick initial pre-alignment; G7: precise initial pre-alignment; G8: best-fit alignment including the entire model surface. M: comparison area of the complete mesh model (excluding the model base). T: comparison area of the teeth only.

Group	N	Trueness (µm)						Precision (µm)					
		Mean	±	SD	Median	±	IQR	Mean	±	SD	Median	±	IQR
G3-T	18	89	±	12	90	±	13	89	±	12	90	±	12
G4A-T	18	89	±	12	90	±	13	89	±	12	90	±	12
G4B-T	18	89	±	12	90	±	13	89	±	12	90	±	12
G5A-T	18	89	±	12	90	±	13	89	±	12	90	±	12
G5B-T	18	89	±	12	90	±	12	89	±	12	90	±	12
G5C-T	18	89	±	12	90	±	13	89	±	12	90	±	12
G6-T	18	91	±	12	92	±	14	90	±	12	92	±	13
G7-T	18	91	±	12	92	±	14	90	±	12	92	±	13
G1A-T	18	91	±	12	92	±	14	90	±	12	92	±	13
G1B-T	18	91	±	12	92	±	14	90	±	12	92	±	13
G1C-T	18	91	±	12	92	±	14	90	±	12	92	±	13
G8-T	18	91	±	12	92	±	15	90	±	12	92	±	14
G4C-T	18	92	±	16	92	±	14	91	±	15	92	±	14
G8-M	18	97	±	17	92	±	27	96	±	17	92	±	25
G1A-M	18	97	±	17	93	±	26	96	±	17	92	±	25
G1B-M	18	97	±	17	93	±	26	96	±	17	92	±	25
G1C-M	18	97	±	17	93	±	26	96	±	17	92	±	25
G6-M	18	97	±	17	93	±	26	96	±	17	92	±	25
G7-M	18	97	±	17	93	±	26	96	±	17	92	±	25
G5C-M	18	98	±	17	94	±	25	98	±	17	94	±	23
G3-M	18	98	±	17	94	±	25	98	±	17	94	±	23
G4A-M	18	98	±	17	94	±	25	98	±	17	94	±	23
G4B-M	18	98	±	17	94	±	25	98	±	17	94	±	23
G4C-M	18	98	±	17	94	±	25	98	±	17	94	±	23
G5A-M	18	98	±	17	94	±	25	98	±	17	94	±	23
G5B-M	18	101	±	19	97	±	19	101	±	18	97	±	17
G2C-T	18	104	±	11	103	±	20	100	±	12	98	±	21
G2A-T	18	113	±	22	108	±	27	111	±	23	107	±	29
G2C-M	18	115	±	16	114	±	21	109	±	16	110	±	20
G2B-T	18	116	±	27	107	±	38	115	±	29	104	±	40
G2A-M	18	122	±	22	117	±	29	119	±	22	111	±	24
G2B-M	18	129		29	123		36	126		30	116		38

TABLE 3. Mean differences (95% CI) of trueness (below the diagonal) and precision (above the diagonal) in microns among all superimposition methods. Statistically significant differences (*p>.05*) are highlighted in bold and marked with an asterisk (*). G1A: 3 close-point landmark-based alignment; G1B: 3 distant-point landmark-based alignment; G1C: 7-point landmark-based alignment; G2A: partial area-based alignment of one tooth; G2B: partial area-based alignment of three adjacent teeth; G2C: partial area-based alignment of the palatal rugae; G3: entire tooth area-based alignment; G4A: primary 3 close-point landmark-based alignment followed by a secondary entire tooth area-based alignment; G4B: primary 3 distant-point landmark-based alignment followed by a secondary entire tooth area-based alignment; G4C: primary 7-points landmark-based alignment followed by a secondary entire tooth area-based alignment; G5A: primary partial tooth area-based alignment of one tooth followed by a secondary entire tooth area-based alignment; G5B: primary partial area-based alignment of three adjacent teeth followed by a secondary entire tooth area-based alignment; G5C: primary partial area-based alignment of the palatal rugae followed by a secondary entire tooth area-based alignment; G6: quick initial pre-alignment; G7: precise initial pre-alignment; G8: best-fit alignment including the entire model surface. M: comparison area of the complete mesh model (excluding the model base). T: comparison area of the teeth only.

G1A-T	G1A-T	6 (-15 , 27)	0 (-21 , 21)	6 (-15 , 27)	0 (-21 , 21)	6 (-15 , 27)	21 (0 , 42)*	**29 (8 , 50)***	G1A-T
G1A-M	6 (-15 , 27)	G1A-M	6 (-15 ,27)	0 (-21 , 21)	6 (-15 ,27)	0 (-21 , 21)	15 (-6 , 36)	**23 (2 , 44)***	G1A-M
G1B-T	0 (-21 , 21)	6 (-15 , 27)	G1B-T	6 (-15 , 27)	0 (-21 , 21)	6 (-15 , 27)	21 (0 , 42)*	**29 (8 , 50)***	G1B-T
G1B-M	6 (-15 , 27)	0 (-21 , 21)	6 (-15 , 27)	G1B-M	6 (-15 , 27)	0 (-21 , 21)	15 (-6 , 36)	**23 (2 , 44)***	G1B-M
G1C-T	0 (-21 , 21)	6 (-15 , 27)	0 (-21 , 21)	6 (-15 , 27)	G1C-T	6 (-15 , 27)	21 (0 , 42)*	**29 (8 , 50)***	G1C-T
G1C-M	6 (-15 , 27)	0 (-21 , 21)	6 (-15 , 27)	0 (-21 , 21)	6 (-15 , 27)	G1C-M	15 (-6 , 36)	23 (2 , 44)	G1C-M
G2A-T	**22 (1 , 43)***	16 (5 , 37)	**22 (1 , 43)***	16 (-5 , 37)	**22 (1 , 43)***	16 (-5 , 37)	G2A-T	8 (-13 , 29)	G2A-T
G2A-M	**32 (11 , 52)***	**26 (5 , 47)***	**32 (11 , 52)***	**26 (5 , 47)***	**32 (11 , 52)***	**26 (5 , 47)***	9 (-11 , 33)	G2A-M	G2A-M
G2B-T	**25 (4 , 46)***	19 (-2 , 40)	**25 (4 , 46)***	19 (-2 , 40)	**25 (4 , 46)***	19 (-2 , 40)	3 (-18 , 24)	6 (-14 , 27)	G2B-T
G2B-M	**38 (17 , 59)***	**32 (-11 , 53)***	**38 (17 , 59)***	**32 (11 , 53)***	**38 (17 , 59)***	**32 (11 , 53)***	16 (-5 , 37)	7 (-14 , 27)	G2B-M
G2C-T	13 (-8 , 34)	7 (-14 , 28)	13 (-8 , 34)	7 (-14 , 28)	13 (-8 , 34)	7 (-14 , 28)	9 (-11 , 33)	19 (-2 , 40)	G2C-T
G2C-M	**24 (3 , 45)***	18(-3, 39)	**24 (3 , 45)***	18 (-3 , 39)	**24 (3 , 45)***	18 (-3 , 39)	2 (-19 , 23)	8 (-13 , 29)	G2C-M
G3-T	2 (-19 , 23)	8 (-13 , 28)	2 (-19 , 23)	8 (-13 , 28)	2 (-19 , 23)	8 (-13 , 28)	**24 (3 , 45)***	**33 (12 , 54)***	G3-T
G3-M	7 (-14 , 28)	1 (-20 , 22)	7 (-14 , 28)	1 (-20 , 22)	7 (-14 , 28)	1 (-20 , 22)	15 (-6 , 36)	**25 (5 , 45)***	G3-M
G4A-T	2 (-19 , 23)	8 (-13, 28)	2 (-19 , 23)	4 (-13 , 28)	2 (-19 , 23)	8 (-13 , 28)	**24 (3 , 45)***	**33 (12 , 54)***	G4A-T
G4A-M	7 (-14 , 28)	1 (-20, 22)	7 (-14 , 28)	1 (-20 , 20)	7 (14 , 28)	1 (-20 , 22)	15 (-6 , 36)	**25 (4 , 45)***	G4A-M
G4B-T	2 (-19 , 23)	8 (-13 , 28)	2 (-19 , 23)	8 (-13 , 28)	2 (-19 , 23)	8 (-13 , 28)	**24 (3 , 45)***	**33 (12 , 54)***	G4B-T
G4B-M	7 (-14 , 28)	1 (-20 , 22)	7 (-14 , 28)	1 (-20 , 22)	7 (-14 , 28)	1 (-20 , 22)	15 (-6 , 36)	**25 (4 , 45)***	G4B-M
G4C-T	1 (-20 , 22)	5 (-16 , 26)	1 (-20 , 22)	5 (-16 , 26)	1 (-20 , 22)	5 (-16 , 26)	**21 (0 , 42)***	**31 (10 , 52)***	G4C-T
G4C-M	7 (-14 , 28)	1 (-20 , 22)	7 (-14 , 28)	1 (-21 , 22)	7 (-14 , 28)	1 (-20 , 22)	15 (-6 , 36)	**25 (4 , 45)***	G4C-M
G5A-T	2 (-19 , 23)	8 (-13 , 28)	2 (-1 , 23)	8 (-13 , 28)	2 (-19 , 23)	8 (-13 , 28)	**24 (3 , 45)***	**33 (12 , 54)***	G5A-T
G5A-M	7 (-14 , 28)	1 (-20 , 22)	7 (-14 , 28)	1 (-20 , 22)	7 (-14 , 28)	1 (-20 , 22)	15 (-6 , 36)	**24 (4 , 45)***	G5A-M
G5B-T	2 (-19 , 23)	8 (-13 , 28)	2 (-19 , 23)	8 (-13 , 28)	5 (-19 , 23)	8 (-13 , 28)	**24 (3 , 45)***	**33 (12 , 54)***	G5B-T
G5B-M	10 (-11 , 31)	4 (-17 , 25)	10 (-11 , 31)	4 (-17 , 25)	10 (-11 , 31)	4 (-17 , 25)	12 (-9 , 33)	**21 (0 , 42)***	G5B-M
G5C-T	2 (-19 , 23)	8 (-13 , 28)	2 (-19 , 23)	8 (-13 , 28)	2 (-19 , 23)	8 (-13 , 28)	**24 (3 , 45)***	**33 (12 , 54)***	G5C-T
G5C-M	7 (-14 , 28)	1 (-20 , 22)	7 (-14 , 28)	1 (-20 , 22)	7 (-14 , 28)	1 (-20 , 22)	15 (-6 , 36)	**25 (4 , 45)***	G5C-M
G6-T	0 (-21 , 21)	6 (-15 , 27)	0 (-21 , 21)	6 (-15 , 27)	0 (-21 , 21)	6 (-15 , 27)	**22 (1 , 43)***	**32 (11 , 52)***	G6-T
G6-M	6 (-15 , 27)	0 (-21 , 21)	6 (-15 , 27)	0 (-21 , 21)	6 (-15 , 27)	0 (-21 , 21)	16 (-5 , 37)	**26 (5 , 47)***	G6-M
G7-T	0 (-21 , 21)	6 (-15 , 27)	0 (-21 , 21)	6 (-15 , 25)	0 (-21 , 21)	6 (-15 , 27)	**22 (1 , 43)***	**32 (11 , 52)***	G7-T
G7-M	6 (-15 , 27)	0 (-21 , 21)	6 (-15 , 27)	0 (-21 , 21)	6 (-15 , 27)	0 (-21 , 21)	16 (-5 , 37)	**26 (5 , 47)***	G7-M
G8-T	0 (-21 , 21)	6 (-15 , 27)	0 (-21 , 21)	6 (-15 , 27)	0 (-21 , 21)	6 (-15 , 27)	**22 (1 , 43)***	**31 (11 , 52)***	G8-T
G8-M	6 (-15 , 27)	0 (-21 , 21)	6 (-15 , 27)	0 (-21 , 21)	6 (-15 , 27)	0 (-21 , 21)	16 (-5 , 37)	**26 (5 , 47)***	G8-M

TABLE 3. (Continued)

G1A-T	**25 (4 , 46)***	**36 (15 , 57)***	10 (-11 , 31)	18 (-3 , 40)	2 (-20 , 23)	7 (-14 , 28)	2 (-20 , 23)	7 (-14 , 28)	G1A-T
G1A-M	19 (-3 , 40)	**29 (8 , 51)***	4 (-17 , 25)	12 (-9 , 33)	8 (-13 , 29)	1 (-20 , 22)	8 (-13 , 29)	1 (-20 , 22)	G1A-M
G1B-T	**25 (4 , 46)***	**36 (15 , 57)***	10 (-11 , 31)	18 (-3 , 40)	2 (-20 , 23)	7 (-14 , 28)	2 (-20 , 23)	7 (-14 , 28)	G1B-T
G1B-M	19 (-3 , 40)	**29 (8 , 51)***	4 (-17 , 25)	12 (-9 , 33)	8 (-13 ,29)	1 (-20 , 22)	8 (-13 ,29)	1 (-20 , 22)	G1B-M
G1C-T	**25 (4 , 46)***	**36 (15 , 57)***	10 (-11 , 31)	18 (-3 , 40)	2 (-20 , 23)	7 (-14 , 28)	2 (-20 , 23)	7 (-14 , 28)	G1C-T
G1C-M	19 (-3 , 40)	**29 (8 , 51)***	4 (-17 , 25)	12 (-9 , 33)	8 (-13 ,29)	1 (-20 , 22)	2 (-20 ,23)	1 (-20 , 22)	G1C-M
G2A-T	4 (-17 , 25)	15 (-6 , 36)	11 (-10 , 32)	2 (-19 , 23)	22 (1 , 44)	14 (-7 , 35)	22 (1 , 44)	14 (-7 , 35)	G2A-T
G2A-M	4 (-17 , 25)	7 (-14 , 28)	19 (-2 , 40)	11 (-11 , 32)	**31 (9 , 52)***	22 (1 , 43)	**31 (9 , 52)***	22 (1 , 43)	G2A-M
G2B-T	G2B-T	11 (-10 , 32)	15 (-6, 36)	6 (-15 , 27)	**26 (5 , 47)***	17 (-4 , 38)	**26 (5 , 47)***	17 (-4 , 38)	G2B-T
G2B-M	13 (-8 , 34)	G2B-M	**26 (5 , 47)***	17 (-4 , 38)	**37 (16 , 58)***	**28 (7 , 49)***	**37 (16 , 58)***	**28 (7 , 49)***	G2B-M
G2C-T	13 (-8 , 33)	**26 (5 , 46)***	G2C-T	9 (-12 , 30)	11 (-10 , 32)	3 (-19 , 24)	11 (-10 , 32)	3 (-19 , 24)	G2C-T
G2C-M	1 (-19 , 22)	14 (-7 , 35)	11 (-10 , 32)	G2C-M	20 (-1 , 41)	11 (-10 , 32)	20 (-1 , 41)	11 (-10 , 32)	G2C-M
G3-T	**27 (6 , 48)***	**40 (19 , 61)***	14 (-7 , 35)	**25 (5 , 46)***	G3-T	9 (-12 , 30)	0 (-21 , 21)	9 (-12 , 30)	G3-T
G3-M	18 (-3 , 39)	**31 (10 , 52)***	6 (-15 , 27)	18 (-3 , 39)	9 (-12 , 30)	G3-M	9 (-12 , 30)	0 (-21 , 21)	G3-M
G4A-T	**27 (6 , 48)***	**40 (19 , 61)***	14 (-7 , 35)	**25 (5 , 46)***	0 (-21 , 21)	9 (-12 , 30)	G4A-T	9 (-12 , 30)	G4A-T
G4A-M	18 (-3 , 39)	**31 (10 , 52)***	6 (-15 , 27)	18 (-3 , 39)	9 (-12 , 30)	0 (-21 , 21)	9 (-12 , 30)	G4A-M	G4A-M
G4B-T	**27 (6 , 48)***	**40 (19 , 61)***	14 (-7 , 35)	**25 (5 , 46)***	0 (-21 , 21)	9 (-12 , 30)	0 (-21 , 21)	9 (-12 , 30)	G4B-T
G4B-M	18 (-3 , 39)	**31 (10 , 52)***	6 (-15 , 27)	18 (-3 , 39)	9 (-12 , 30)	0 (-21 , 21)	9 (-12 , 30)	0 (-21 , 21)	G4B-M
G4C-T	**24 (3 , 45)***	**40 (19 , 61)***	12 (-9 , 33)	**23 (2 , 44)***	6 (-15 , 27)	6 (-15 , 27)	3 (-18 , 23)	6 (-15 , 27)	G4C-T
G4C-M	18 (-3 , 39)	**31 (10 , 52)***	6 (-15 , 27)	18 (-3 , 39)	9 (-12 , 30)	0 (-21 , 21)	9 (-12 , 30)	0 (-21 , 21)	G4C-M
G5A-T	**27 (6 , 48)***	**40 (19 , 61)***	14 (-7 , 35)	**25 (5 , 46)***	0 (-21 , 21)	9 (-12 , 30)	0 (-21 , 21)	9 (-12 , 30)	G5A-T
G5A-M	18 (-3 , 39)	**31 (10 , 52)***	6 (-15 , 26)	18 (-3 , 39)	9 (-12 , 30)	0 (-21 , 21)	9 (-12 , 30)	0 (-21 , 21)	G5A-M
G5B-T	**27 (6 , 48)***	**40 (19 , 61)***	14 (-7 , 35)	**25 (5 , 46)***	0 (-21 , 21)	9 (-12 , 30)	0 (-21 , 21)	9 (-12 , 30)	G5B-T
G5B-M	15 (-6 , 36)	**28 (7 , 49)***	2 (-18 , 23)	14 (-7 , 34)	12 (-19 , 33)	3 (-18 , 24)	12 (-19 , 33)	3 (-18 , 24)	G5B-M
G5C-T	**27 (6 , 48)***	**40 (19 , 61)***	14 (-7 , 35)	**25 (5 , 46)***	0 (-21 , 21)	9 (-12 , 30)	0 (-21 , 21)	9 (-12 , 30)	G5C-T
G5C-M	18 (-3 , 39)	**31 (10 , 52)***	6 (-15 , 27)	17 (-4 , 38)	9 (-12 , 30)	0 (-21 , 21)	9 (-12 , 30)	0 (-21 , 21)	G5C-M
G6-T	**25 (4 , 46)***	**38 (17 , 59)***	13 (-8 , 34)	**24 (3 , 45)***	7 (-14 , 28)	7 (-14 , 28)	2 (-19 , 23)	7 (-14 , 28)	G6-T
G6-M	19 (-2 , 40)	**32 (11 , 53)***	7 (-14 , 28)	18 (-3 , 39)	1 (-20 , 22)	1 (-20 , 22)	8 (-13 , 28)	1 (-20 , 22)	G6-M
G7-T	**25 (4 , 46)***	**38 (17 , 59)***	13 (-8 , 34)	**24 (3 , 45)***	7 (-14 , 28)	7 (-14 , 28)	2 (-19 , 23)	7 (-14 , 28)	G7-T
G7-M	19 (-2 , 40)	**32 (11 , 53)***	7 (-14 , 28)	18 (-3 , 39)	1 (-20 , 22)	1 (-20 , 22)	8 (-13 , 28)	1 (-20 , 22)	G7-M
G8-T	**25 (4 , 46)***	**38 (17 , 59)***	13 (-8 , 33)	**24 (3 , 45)***	7 (-14 , 28)	7 (-14 , 28)	2 (-19 , 23)	7 (-14 , 28)	G8-T
G8-M	19 (-1 , 40)	**32 (11 , 53)***	7 (-14 , 28)	18 (-3 , 39)	1 (-20 , 22)	1 (-20 , 22)	8 (-13 , 28)	1 (-20 , 22)	G8-M

TABLE 3. (Continued)

G1A-T	2 (-20 , 23)	7 (-14 , 28)	1 (-20 , 22)	7 (-14 , 29)	2 (-20 , 23)	7 (-14 , 29)	2 (-20 , 23)	10 (-11 , 31)	G1A-T
G1A-M	8 (-13 , 29)	1 (-20 , 22)	5 (-16 , 26)	1 (-20 , 22)	8 (-13 , 29)	1 (-20 , 22)	8 (-13 , 29)	4 (-17 , 25)	G1A-M
G1B-T	2 (-20 , 23)	7 (-14 , 28)	1 (-20 , 22)	7 (-14 , 28)	2 (-20 , 23)	7 (-14 , 29)	2 (-20 , 23)	10 (-11 , 31)	G1B-T
G1B-M	8 (-13 ,29)	1 (-20 , 22)	5 (-16 , 26)	1 (-20 , 22)	8 (-13 ,29)	1 (-20 , 22)	8 (-13 ,29)	4 (-17 , 25)	G1B-M
G1C-T	2 (-20 , 23)	7 (-14 , 28)	1 (-20 , 22)	7 (-14 , 28)	2 (-20 , 23)	7 (-14 , 29)	2 (-20 , 23)	10 (-11 , 31)	G1C-T
G1C-M	8 (-13 ,29)	1 (-20 , 22)	5 (-16 , 26)	1 (-20 , 22)	8 (-13 ,29)	1 (-20 , 22)	8 (-13 ,29)	4 (-17 , 25)	G1C-M
G2A-T	22 (1 , 44)	14 (-7 , 35)	20 (-1 , 41)	14 (-7 , 35)	22 (1 , 44)	13 (-8 , 35)	22 (1 , 44)	11 (-11 , 32)	G2A-T
G2A-M	**31 (9 , 52)***	22 (1 , 43)	**28 (7 , 49)***	22 (1 , 43)	**31 (9 , 52)***	22 (1 , 43)	**31 (9 , 52)***	19 (-2 , 40)	G2A-M
G2B-T	**26 (5 , 47)***	17 (-4 , 38)	**24 (3 , 45)***	17 (-4 , 38)	**26 (5 , 47)***	17 (-4 , 38)	**26 (5 , 47)***	14 (-7 , 35)	G2B-T
G2B-M	**37 (16 , 58)***	**28 (7 , 49)***	**35 (14 , 56)***	**28 (7 , 49)***	**37 (16 , 58)***	**28 (7 , 49)***	**37 (16 , 58)***	**25 (4 , 46)***	G2B-M
G2C-T	11 (-10 , 32)	3 (-19 , 24)	9 (-12 , 30)	3 (-19 , 24)	11 (-10 , 32)	2 (-19 , 24)	11 (-10 , 32)	1 (-21 , 22)	G2C-T
G2C-M	20 (-1 , 41)	11 (-10 , 32)	18 (-4 , 49)	11 (-10 , 32)	20 (-1 , 41)	11 (-10 , 32)	20 (-1 , 41)	8 (-13 , 29)	G2C-M
G3-T	0 (-21 , 21)	9 (-12 , 30)	3 (-19 , 24)	9 (-12 , 30)	0 (-21 , 21)	9 (-12 , 30)	0 (-21 , 21)	12 (-9 , 33)	G3-T
G3-M	9 (-12 , 30)	0 (-21 , 21)	6 (-15 , 27)	0 (-21 , 21)	9 (-12 , 30)	0 (-21 , 21)	9 (-12 , 30)	3 (-18 , 24)	G3-M
G4A-T	0 (-21 , 21)	9 (-12 , 30)	3 (-19 , 24)	9 (-12 , 30)	0 (-21 , 21)	9 (-12 , 30)	0 (-21 , 21)	12 (-9 , 33)	G4A-T
G4A-M	9 (-12 , 30)	0 (-21 , 21)	6 (-15 , 27)	0 (-21 , 21)	9 (-12 , 30)	0 (-21 , 21)	9 (-12 , 30)	3 (-18 , 24)	G4A-M
G4B-T	G4B-T	9 (-12 , 30)	3 (-19 , 24)	9 (-12 , 30)	0 (-21 , 21)	9 (-12 , 30)	0 (-21 , 21)	12 (-9 , 33)	G4B-T
G4B-M	9 (-12 , 30)	G4B-M	6 (-15 , 27)	0 (-21 , 21)	9 (-12 , 30)	0 (-21 , 21)	9 (-12 , 30)	3 (-18 , 24)	G4B-M
G4C-T	3 (-18 , 23)	6 (-15 , 27)	G4C-T	6 (-15 , 27)	2 (-19 , 24)	6 (-15 , 27)	2 (-19 , 24)	9 (-12 , 31)	G4C-T
G4C-M	9 (-12 , 30)	0 (-21 , 21)	6 (-15 , 27)	G4C-M	9 (-12 , 30)	0 (-21 , 21)	9 (-12 , 30)	3 (-18 , 24)	G4C-M
G5A-T	0 (-21 , 21)	9 (-12 , 30)	3 (-18 , 23)	9 (-12 , 30)	G5A-T	9 (-12 , 30)	0 (-21 , 21)	12 (-9 , 33)	G5A-T
G5A-M	9 (-12 , 30)	0 (-21 , 21)	6 (-15 , 27)	0 (-21 , 21)	9 (-12 , 30)	G5A-M	9 (-12 , 30)	3 (-18 , 24)	G5A-M
G5B-T	0 (-21 , 21)	9 (-12 , 30)	3 (-18 , 23)	9 (-12 , 30)	0 (-21 , 21)	9 (-12 , 30)	G5B-T	12 (-9 , 33)	G5B-T
G5B-M	12 (-9 , 33)	3 (-18 , 24)	9 (-12 , 30)	3 (-18 , 24)	12 (-9 , 33)	3 (-18 , 24)	12 (-9 , 33)	G5B-M	G5B-M
G5C-T	0 (-21 , 21)	9 (-12 , 30)	3 (-18 , 23)	9 (-12 , 30)	0 (-21 , 21)	9 (-12 , 30)	0 (-21 , 21)	12 (-9 , 33)	G5C-T
G5C-M	9 (-12 , 30)	0 (-21 , 21)	6 (-15 , 27)	0 (-21 , 21)	9 (-12 , 30)	0 (-21 , 21)	9 (-12 , 30)	3 (-18 , 23)	G5C-M
G6-T	2 (-19 , 23)	7 (-14 , 28)	1 (-20 , 22)	7 (-14 , 28)	2 (-19 , 23)	7 (-14 , 28)	2 (-19 , 23)	10 (-11 , 31)	G6-T
G6-M	8 (-13 , 28)	1 (-20 , 22)	5 (-16 , 26)	1 (-20 , 22)	8 (-13 , 28)	1 (-20 , 22)	8 (-13 , 28)	4 (-17 , 25)	G6-M
G7-T	2 (-19, 23)	7 (-14 , 28)	1 (-20 , 22)	7 (-14 , 28)	2 (-19 , 23)	7 (-14 , 28)	2 (-19 , 23)	10 (-11 , 31)	G7-T
G7-M	8 (-13 , 28)	1 (-20 , 22)	5 (-16 , 26)	1 (-20 , 22)	8 (-13 , 28)	1 (-20 , 22)	8 (-13 , 28)	4 (-17 , 25)	G7-M
G8-T	2 (-19, 23)	7 (-14 , 28)	1 (-20 , 22)	7 (-14 , 28)	2 (-19 , 23)	7 (-14 , 28)	2 (-19 , 23)	10 (-11 , 31)	G8-T
G8-M	7 (-13 , 28)	1 (-20 , 22)	5 (-16 , 26)	1 (-20 , 22)	7 (-13 , 28)	1 (-20 , 22)	2 (-19 , 23)	4 (-16 , 25)	G8-M

TABLE 3. (Continued)

G1A-T	2 (-20 , 23)	7 (-14 , 29)	0 (-21 , 21)	6 (-15 , 27)	0 (-21 , 21)	6 (-15 , 27)	0 (-21 , 21)	6 (-15 , 27)	G1A-T
G1A-M	8 (-13 , 29)	1 (-20 , 22)	6 (-15 , 27)	0 (-21 , 21)	6 (-15 , 27)	0 (-21 , 21)	6 (-15 , 27)	0 (-21 , 21)	G1A-M
G1B-T	2 (-20 , 23)	7 (-14 , 28)	0 (-21 , 21)	6 (-15 , 27)	0 (-21 , 21)	6 (-15 , 27)	0 (-21 , 21)	6 (-15 , 27)	G1B-T
G1B-M	8 (-13 ,29)	1 (-20 , 22)	6 (-15 , 27)	0 (-21 , 21)	6 (-15 , 27)	0 (-21 , 21)	6 (-15 , 27)	0 (-21 , 21)	G1B-M
G1C-T	2 (-20 , 23)	7 (-14 , 28)	0 (-21 , 21)	6 (-15 , 27)	0 (-21 , 21)	6 (-15 , 27)	0 (-21 , 21)	6 (-15 , 27)	G1C-T
G1C-M	8 (-13 ,29)	1 (-20 , 22)	6 (-15 , 27)	0 (-21 , 21)	6 (-15 , 27)	0 (-21 , 21)	6 (-15 , 27)	0 (-21 , 21)	G1C-M
G2A-T	22 (1 , 44)	14 (-7 , 35)	21 (0 , 42)	15 (-6 , 36)	21 (0 , 42)	15 (-6 , 36)	21 (0 , 42)	15 (-6 , 36)	G2A-T
G2A-M	**31 (9 , 52)***	22 (1 , 43)	**29 (8 , 50)***	**23 (2 , 44)***	**29 (8 , 50)***	**23 (2 , 44)***	**29 (8 , 50)***	**23 (2 , 44)***	G2A-M
G2B-T	**26 (5 , 47)***	17 (-4 , 39)	**25 (4 , 46)***	19 (-3 , 40)	**25 (4 , 46)***	19 (-3 , 40)	**25 (4 , 46)***	19 (-3 , 40)	G2B-T
G2B-M	**37 (16 , 58)***	**28 (7 , 49)***	**36 (15 , 57)***	**29 (8 , 51)***	**36 (15 , 57)***	**29 (8 , 51)***	**35 (14 , 57)***	**29 (8 , 51)***	G2B-M
G2C-T	11 (-10 , 32)	3 (-18 , 24)	10 (-11 , 31)	4 (-17 , 25)	10 (-11 , 31)	4 (-17 , 25)	10 (-11 , 31)	4 (-17 , 25)	G2C-T
G2C-M	20 (-1 , 41)	11 (-10 , 32)	18 (-3 , 40)	12 (-9 , 33)	18 (-3 , 40)	12 (-9 , 33)	18 (-3 , 39)	12 (-9 , 33)	G2C-M
G3-T	0 (-21 , 21)	9 (-12 , 30)	2 (-20 , 23)	8 (-13 , 29)	2 (-20 , 23)	8 (-13 , 29)	2 (-19 , 23)	8 (-13 , 29)	G3-T
G3-M	9 (-12 , 30)	0 (-21 , 21)	7 (-14 , 28)	1 (-20 , 22)	7 (-14 , 28)	1 (-20 , 22)	7 (-14 , 28)	1 (-20 , 22)	G3-M
G4A-T	0 (-21 , 21)	9 (-12 , 30)	2 (-20 , 23)	8 (-13 , 29)	2 (-20 , 23)	8 (-13 , 29)	2 (-19 , 23)	8 (-13 , 29)	G4A-T
G4A-M	9 (-12 , 30)	0 (-21 , 21)	7 (-14 , 28)	1 (-20 , 22)	7 (-14 , 28)	1 (-20 , 22)	7 (-14 , 28)	1 (-20 , 22)	G4A-M
G4B-T	0 (-21 , 21)	9 (-12 , 30)	2 (-20 , 23)	8 (-13 , 29)	2 (-20 , 23)	8 (-13 , 29)	2 (-19 , 23)	8 (-13 , 29)	G4B-T
G4B-M	9 (-12 , 30)	0 (-21 , 21)	7 (-14 , 28)	1 (-20 , 22)	7 (-14 , 28)	1 (-20 , 22)	7 (-14 , 28)	1 (-20 , 22)	G4B-M
G4C-T	3 (-19 , 24)	6 (-15 , 27)	1 (-20 , 22)	5 (-16 , 26)	1 (-20 , 22)	5 (-16 , 26)	1 (-20 , 22)	5 (-16 , 26)	G4C-T
G4C-M	9 (-12 , 30)	0 (-21 , 21)	7 (-14 , 28)	1 (-20 , 22)	7 (-14 , 28)	1 (-20 , 22)	7 (-14 , 28)	1 (-20 , 22)	G4C-M
G5A-T	0 (-21 , 21)	9 (-12 , 30)	2 (-20 , 23)	8 (-13 , 29)	2 (-20 , 23)	8 (-13 , 29)	2 (-19 , 23)	8 (-13 , 29)	G5A-T
G5A-M	9 (-12 , 30)	0 (-21 , 21)	7 (-14 , 28)	1 (-20 , 22)	7 (-14 , 28)	1 (-20 , 22)	7 (-14 , 28)	1 (-20 , 22)	G5A-M
G5B-T	0 (-21 , 21)	9 (-12 , 30)	2 (-20 , 23)	8 (-13 , 29)	2 (-20 , 23)	8 (-13 , 29)	2 (-19 , 23)	8 (-13 , 29)	G5B-T
G5B-M	12 (-9 , 33)	3 (-18 , 24)	10 (-11 , 31)	4 (-17 , 25)	10 (-11 , 31)	4 (-17 , 25)	10 (-11 , 31)	4 (-17 , 25)	G5B-M
G5C-T	G5C-T	9 (-12 , 30)	2 (-20 , 23)	8 (-13 , 29)	2 (-20 , 23)	8 (-13 , 29)	2 (-19 , 23)	8 (-13 , 29)	G5C-T
G5C-M	9 (-12 , 30)	G5C-M	7 (-14 , 28)	1 (-20 , 22)	7 (-14 , 28)	1 (-20 , 22)	7 (-14 , 28)	1 (-20 , 22)	G5C-M
G6-T	2 (-19 , 23)	7 (-14 , 28)	G6-T	6 (-15 , 27)	6 (-15 , 27)	0 (-21 , 21)	6 (-15 , 27)	0 (-21 , 21)	G6-T
G6-M	8 (-13 , 28)	1 (-20 , 22)	6 (-15 , 27)	G6-M	6 (-15 , 27)	0 (-21 , 21)	6 (-15 , 27)	0 (-21 , 21)	G6-M
G7-T	2 (-19 , 23)	7 (-14 , 28)	6 (-15 , 27)	6 (-15 , 27)	G7-T	6 (-15 , 27)	0 (-21 , 21)	6 (-15 , 27)	G7-T
G7-M	8 (-13 , 28)	1 (-20 , 22)	6 (-15 , 27)	0 (-21 , 21)	6 (-15 , 27)	G7-M	6 (-15 , 27)	0 (-21 , 21)	G7-M
G8-T	2 (-19 , 23)	7 (-14 , 28)	6 (-15 , 27)	6 (-15 , 27)	0 (-21 , 21)	6 (-15 , 27)	G8-T	6 (-15 , 27)	G8-T
G8-M	7 (-13 , 28)	1 (-20 , 22)	6 (-15 , 27)	0 (-21 , 21)	6 (-15 , 27)	0 (-21 , 21)	6 (-15 , 27)	G8-M	G8-M

TABLE 4. Analysis of variance for RMS error.

Source	**DF**	**Partial SS**	**Contribution**	**MS**	***F-value***	***p-value***
Superimposition methods	15	48050.25	23.30%	3203.35	11.79	0.0000
Comparison area	1	9571.36	4.64%	9571.36	35.22	0.0000
Superimposition methods # Comparison area	15	761.42	0.37%	50.76	0.19	0.9997
Residual	544	147852.36	71.69%	271.79		
Total	575	206235.39	100%	358.67		

FIGURES

FIGURE 1. Superimposition methods tested: 3 close-point landmark-based alignment (1a); 3 distant-point landmark-based alignment (1b); 7-point landmark-based alignment (1c); partial area-based alignment of one tooth (2a); partial area-based alignment of adjacent three teeth (2b); partial area-based alignment of the palatal rugae (2c); entire tooth area-based alignment (3); primary 3 close-point landmark-based alignment followed by a secondary entire area-based alignment (4a); primary 3 distant-point landmark-based alignment followed by a secondary entire tooth area-based alignment (4b); primary 7-points landmark-based alignment followed by a secondary entire tooth area-based alignment (4c); primary partial area-based alignment of one tooth followed by a secondary entire tooth area-based alignment (5a); primary partial area-based alignment of three teeth followed by a secondary entire tooth area-based alignment (5b); primary partial area-based alignment of the palatal rugae followed by a secondary entire tooth area-based alignment (5c); quick initial alignment (6); precise initial alignment (7); entire model area-based alignment (8). The light blue dotted texture represents the area on which the area-based superimposition method was based. The grey dotted texture was used to represent the double superimposition method.

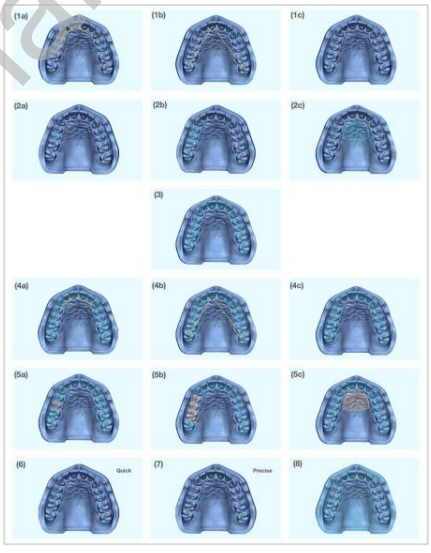

FIGURE 2. Representative color maps of the RMS error discrepancies measured when a partial area-based alignment of one tooth was used, selecting the complete mesh (excluding the model base) (a), or the teeth area (b), as the comparison area. Representative color maps of the RMS error discrepancies measured when an entire tooth area-based alignment was used, selecting the complete mesh excluding the model base (c), or the teeth area (d), as the selected comparison area for accuracy analysis.

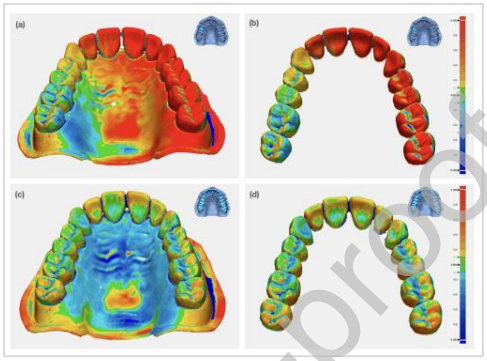

FIGURE 3. Accuracy analysis: box plot graph of trueness values by groups. Identical superscripts indicate statistically significant differences among subgroups.

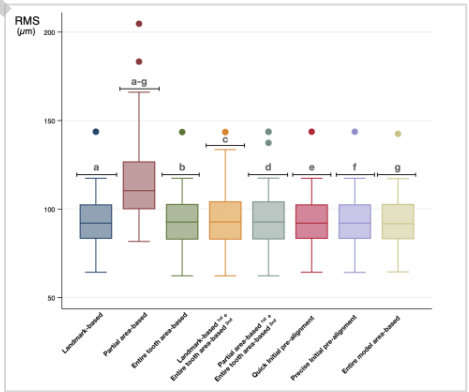

FIGURE 4. Accuracy analysis; box plot graph of trueness values by subgroup. G1A: 3 close-point landmark-based alignment; G1B: 3 distant-point landmark-based alignment; G1C: 7-point landmark-based alignment; G2A: partial area-based alignment of one tooth; G2B: partial area-based alignment of three adjacent teeth; G2C: partial area-based alignment of the palatal rugae; G3: entire tooth area-based alignment; G4A: primary 3 close-point landmark-based alignment followed by a secondary entire tooth area-based alignment; G4B: primary 3 distant-point landmark-based alignment followed by a secondary entire tooth area-based alignment; G4C: primary 7-points landmark-based alignment followed by a secondary entire tooth area-based alignment; G5A: primary partial tooth area-based alignment of one tooth followed by a secondary entire tooth area-based alignment; G5B: primary partial area-based alignment of three adjacent teeth followed by a secondary entire tooth area-based alignment; G5C: primary partial area-based alignment of the palatal rugae followed by a secondary entire tooth area-based alignment; G6: quick initial pre-alignment; G7: precise initial pre-alignment; G8: best-fit alignment including the entire model surface. M: comparison area of the complete mesh model (excluding the model base). T: comparison area of the teeth only.

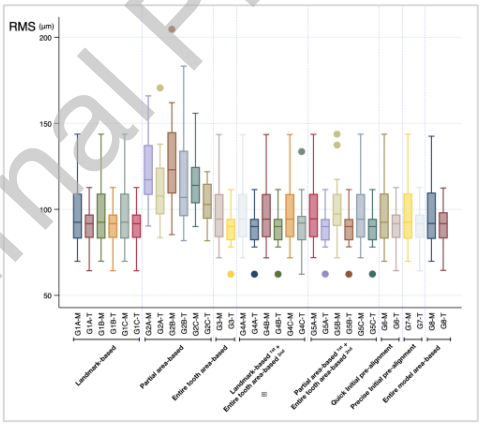

ACKNOWLEDGMENTS

Not applicable.

AUTHOR CONTRIBUTIONS

Alvaro Limones conceived the idea. Alvaro Limones and Gülce Çakmak designed the study. Pedro Molinero-Mourelle acquired the data. Gülce Çakmak and Alvaro Limones analysed the data. Alvaro Limones, Gülce Çakmak and Pedro Molinero-Mourelle led the writing. Alvaro Limones and Silvia Delgado elaborate tables and graphs. Alvaro Limones, Pedro Molinero-Mourelle, Gülce Çakmak, Samir Abou-Ayash, Silvia Delgado, Juan Antonio Martínez Vázquez de Parga, and Alicia Celemín contributed to data interpretation and critically revised the manuscript. All authors gave final approval and agreed to be accountable for all aspects of the scientific work.

FUNDING INFORMATION

Not applicable.

DATA AVAILABILITY STATEMENT

The data that support the findings of this study are available from the corresponding author upon reasonable request.

ETHICS APPROVAL STATEMENT

This in vitro study was exempt from ethics committee approval.

CONFLICT OF INTEREST STATEMENT

The authors have no conflict of interest to report pertaining to the conduction of this study.